

# Antibodies against the erythroferrone N-terminal domain prevent hepcidin suppression and ameliorate murine thalassemia

João Arezes<sup>1\*</sup>, Niall Foy<sup>2\*</sup>, Kirsty McHugh<sup>3</sup>, Doris Quinkert<sup>3</sup>, Susan Benard<sup>4</sup>, Anagha Sawant<sup>5</sup>, Joe N. Frost<sup>1</sup>, Andrew E. Armitage<sup>1</sup>, Sant-Rayn Pasricha<sup>1,6,7</sup>, Pei Jin Lim<sup>1</sup>, May S. Tam<sup>5</sup>, Edward Lavallie<sup>5</sup>, Debra D. Pittman<sup>5</sup>, Orla Cunningham<sup>2</sup>, Matthew Lambert<sup>2</sup>, John E. Murphy<sup>5</sup>, Simon J. Draper<sup>3\*</sup>, Reema Jasuja<sup>5\*</sup> and Hal Drakesmith<sup>1,8\*</sup>

## Affiliations

1. MRC Human Immunology Unit, MRC Weatherall Institute of Molecular Medicine, University of Oxford, John Radcliffe Hospital, Oxford, OX3 9DS, UK
2. BioMedicine Design, Pfizer Biotherapeutics R&D, Dublin D22, Ireland
3. Jenner Institute, University of Oxford, Old Road Campus Research Building, Oxford, OX3 7DQ, UK.
4. BioMedicine Design, Pfizer Biotherapeutics R&D, Cambridge, MA, USA
5. Rare Disease Research Unit, Pfizer Inc., Cambridge, MA, USA
6. Walter and Eliza Hall Institute of Medical Research, Melbourne, Victoria, Australia
7. Department of Medical Biology, The University of Melbourne, Melbourne, Victoria, Australia
8. Haematology Theme Oxford Biomedical Research Centre, Oxford, UK

\* equal contribution

**Short title:** Anti-Erythroferrone antibodies increase hepcidin

**Scientific Category:** Red Cells, Iron and Erythropoiesis

**Abstract word count:** 241

**Text word count:** 4108

**Tables/Figures:** 0 Tables, 6 Figures

**References:** 50

## Correspondence to:

Hal Drakesmith, MRC Human Immunology Unit, MRC Weatherall Institute of Molecular Medicine, University of Oxford, John Radcliffe Hospital, Oxford, OX3 9DS, UK.

Email: alexander.drakesmith@imm.ox.ac.uk

Telephone: +44(0)1865 222415

Fax: +44(0)1865 222406

## Key points

- 1) The N-terminus of ERFE binds BMP6 with nanomolar affinity and is sufficient to inhibit BMP signaling and suppress hepcidin in vivo
- 2) Anti-N-terminal ERFE antibodies prevent Epo-induced hepcidin suppression and decrease iron accumulation and anemia in thalassemic mice

## Abstract

Erythroferrone (ERFE) is produced by erythroblasts in response to erythropoietin (EPO) and acts in the liver to prevent hepcidin stimulation by BMP6. Hepcidin suppression allows for the mobilization of iron to the bone marrow for the production of red blood cells. Aberrantly high circulating ERFE in conditions of stress erythropoiesis, such as in patients with  $\beta$ -thalassemia, promotes the tissue iron accumulation that substantially contributes to morbidity in these patients. Here we developed antibodies against ERFE to prevent hepcidin suppression and correct the iron loading phenotype in a mouse model of  $\beta$ -thalassemia (Hbb(th3/+) mice) and used these antibodies as tools to further characterize ERFE's mechanism of action. We demonstrate that ERFE binds to BMP6 with nanomolar affinity, and binds BMP2 and BMP4 with somewhat weaker affinities. We show that BMP6 binds the N-terminal domain of ERFE, and a polypeptide derived from the N-terminus of ERFE was sufficient to cause hepcidin suppression in Huh7 hepatoma cells and in wildtype mice. Anti-ERFE antibodies targeting the N-terminal domain prevented hepcidin suppression in ERFE-treated Huh7 cells and in EPO-treated mice. Finally, we observed a decrease in splenomegaly and serum and liver iron in anti-ERFE treated Hbb(th3/+) mice, accompanied by an increase in red blood cells and hemoglobin and decrease in reticulocyte counts. In summary, we demonstrate that ERFE binds BMP6 directly and with high affinity, and that antibodies targeting the N-terminal domain of ERFE that prevent ERFE-BMP6 interactions constitute a potential therapeutic tool for iron-loading anemias.

## Introduction

$\beta$ -thalassemia is an inherited hemoglobinopathy characterized by dysfunction or deletion of the  $\beta$  globin genes, leading to haemolytic anemia, ineffective erythropoiesis and iron overload<sup>1,2</sup>. Approximately 1.5% of the population worldwide are carriers of  $\beta$ -thalassemia<sup>3</sup>; homozygous or compound heterozygous states result in thalassaemia intermedia or major (the latter requiring regular blood transfusions)<sup>4</sup>. A main cause of morbidity in these patients is iron overload, which accumulates in several tissues especially the liver, causing damage due to iron toxicity<sup>5</sup>, and is associated with hepatic fibrosis<sup>6</sup> and hepatocellular carcinoma<sup>7,8</sup>; cardiac failure and arrhythmia, endocrine failure (i.e. hypogonadism, diabetes), and osteoporosis<sup>9</sup> may also occur. Current treatments can have undesirable side effects: regular blood transfusions (in thalassemia major) significantly worsens iron accumulation; iron chelators alleviate iron loading, but may require intravenous or subcutaneous administration (although oral administration is also currently used), and may cause gastrointestinal disturbances and/or kidney damage<sup>10</sup>. Understanding the mechanism underlying iron accumulation may contribute to the design of better therapies to improve the clinical outcome.

Enhanced erythropoiesis requires augmented iron availability for heme production<sup>11</sup>. This is achieved by suppression of hepcidin, a hepatic hormone that regulates iron absorption and distribution by inhibiting the iron exporter ferroportin<sup>12-14</sup>. Hepcidin expression is modulated by the BMP/SMAD signalling pathway: binding of Bone Morphogenetic Proteins (BMPs) to BMP receptors in the membrane of hepatocytes causes phosphorylation of cytosolic SMADs (SMAD1/5/8) that translocate to the nucleus complexed with SMAD4 to activate the transcription of target genes, including hepcidin (*HAMP*)<sup>15-17</sup>. This pathway is activated in response to iron via BMP6<sup>18,19</sup>, and by BMP2 independently of BMP6<sup>20</sup>. Hepcidin suppression during erythropoiesis is mediated at least in part by erythroferrone (ERFE), a protein synthesized in erythroblasts in response to erythropoietin (EPO), downstream of JAK2-STAT5 signalling<sup>21</sup>. ERFE inhibits BMP6 and so downregulates BMP/SMAD signalling in hepatocytes<sup>22-24</sup>, thus suppressing hepcidin<sup>24</sup>. ERFE expression is increased in mouse models of  $\beta$ -thalassemia and human thalassemia patients<sup>25,26</sup>. Deletion of the gene *Erfe* (encoding ERFE) in a mouse model of  $\beta$ -thalassemia rescued hepcidin expression and partially decreased the iron accumulation in mice, suggesting that ERFE is a significant contributor to the pathophysiology of the disease<sup>25</sup>. Increased hepcidin activity via injection of minihepcidin (a synthetic hepcidin analogue) has beneficial effects in mouse models of thalassemia intermedia<sup>27</sup> and thalassemia major<sup>28</sup>. Therefore, we sought to develop a therapeutic to block ERFE activity, thus de-repressing hepcidin suppression and reversing iron overload in iron-loading anemias such as  $\beta$ -thalassemia. Here we characterize ERFE binding to different BMPs and demonstrate that the N-terminal domain of ERFE is sufficient for hepcidin suppression. We also developed neutralizing anti-ERFE antibodies that prevent ERFE-mediated hepcidin suppression, *in vitro* and *in vivo*. Finally, we demonstrate that antibodies binding the N-terminal domain of ERFE reduce iron burden and alleviate anemia in a mouse model of  $\beta$ -thalassemia.

## Methods

### Animal studies and treatments

Animal experiments were undertaken under an approved UK Home Office Project License P5AC0E88C9 with ethics approval from the University of Oxford Animal Welfare and Ethical Review Body. All experiments were performed in male mice. Wildtype male C57BL/6 mice were purchased from Envigo, UK. Embryos from Erfe+/- mice on a mixed Sv129/C57BL/6 background were obtained from the Mutant Mouse Regional Resource Center (MMRRC) at UC Davis (strain B6;129S5-Erfetm1Lex/Mmucd, ID MMRRC:032289-UCD) and backcrossed using marker-assisted accelerated backcrossing yielding approximately 99% C57BL/6 background. Heterozygote pairs were mated to generate homozygous animals from which knockout and wild-type colonies were maintained. ERFE knockout mice were used for immunisations. Wildtype and ERFE knockout animals were housed in individually ventilated cages in the Department of Biomedical Services, University of Oxford, and provided access to normal chow (163 ppm of iron, Special Diets Services 801700) and water ad libitum. Hbb(th3/+) mice were obtained from The Jackson Laboratories (JAX, Bar Harbor, ME), bred and maintained at JAX. Age and sex matched Hbb(th3/+) mice were shipped to Pfizer animal facility for experiments and maintained on an iron sufficient diet (67 ppm of iron, Test Diet, 5755). The dietary iron content was lowered in Hbb(th3/+) mice as the higher iron content in standard diet together with ongoing stress erythropoiesis in these mice could lead to unwanted pathology. Iron sufficient diet was also used in wildtype mice when used as control groups for experiments involving Hbb(th3/+) mice. For ERFE treatments in wildtype mice, 8-week old mice were injected intravenously with 100µg of human ERFE (F2 construct) or saline (vehicle) and euthanized 3h after treatment. For antibody testing in erythropoietin (EPO) treated mice, wildtype mice were injected intraperitoneally with 200 IU of recombinant human EPO (Bio-Rad) in water, alone or in combination with intravenous injection of anti-ERFE antibodies (5mg/kg). Two different regimens were used: a) one simultaneous injection of EPO and antibody and cull 18h after treatments or b) daily EPO injections for three consecutive days, with simultaneous antibody treatment on days 1 and 3, and cull 24h after the last EPO injection. In both cases, the control groups used were non-EPO treated mice (vehicle + IgG antibody control) and EPO-treated with IgG antibody control. For antibody testing in Hbb(th3/+) mice, four-weeks old mice were treated intravenously with 5mg/kg of IgG2A control antibody, anti-ERFE 15.1 or anti-ERFE 20.1, twice a week for four or eight weeks. IgG2A-treated WT mice were used as control for baseline levels in the 4 weeks experiment. After 4 or 8 weeks of treatment mice were euthanized for analysis of serum and liver iron. Mice were euthanized in increasing CO<sub>2</sub> concentrations.

### Protein production

Expi293F™ cells (Gibco A14527) were propagated in Expi293 expression medium at 36°C and transfected with intact expression vector DNA (human or mouse ERFE) according to manufacturer's recommended protocols. Following transfection, the cell culture was returned to 8% CO<sub>2</sub> shaking incubator at 36°C. No supplementary tryptone feed was given to these cultures. Conditioned media (CM) was collected 120 hours post-transfection. CM was transferred to sterile 1L Nalgene bottles and centrifuged for 6min at 1800 RPM, 4°C in Sorvall H-6000A rotor (940x g). Clarified CM was collected and filtered using Sartopore 2XL 0.8/0.2 µm filtration. ERFE proteins were linked to monoFc<sup>29</sup> using a G4S linker at the N-terminus. The recombinant monoFc-huERFE (human) and monoFc-muERFE (murine) were purified in the following manner. All chromatography steps were

performed at 4°C. The proteins were captured from CM using MabSelect SuRe (GE Healthcare), washed extensively with Calcium-Magnesium-free PBS (PBS-CMF) pH 7.2, and eluted with a decreasing pH gradient. Fractions containing ERFE were exchanged into low sodium chloride pH 8.0 buffer, loaded onto a Q Sepharose HP column (GE Healthcare), and an increasing sodium chloride gradient elution was performed. A Hiload Superdex 200 column (GE Healthcare) was used as a final purification step with mobile phase containing Arginine pH 7.0. Fractions with high purity of ERFE were pooled and buffer exchanged into PBS-CMF pH7.2. Analysis of the ERFE sequence indicates the presence of two potential furin cleavage sites, at positions 42 and 212. Constructs were designed based on all the potential furin cleavage variants that could exist assuming cleavage by furin at both sites. This resulted in 5 furin cleavage constructs being produced (see Figure 2). These constructs were linked to monoFc<sup>29</sup> using a G4S linker at the N-terminus. Furin subunit constructs were expressed and purified as previously described. Sequences are available upon request.

#### **Antibody discovery: Naïve Human Phage library approach**

An antibody scFv phage display library (WyHN5) was used to screen for binders to ERFE. Four rounds of selection with decreasing antigen concentration were carried out using biotinylated ERFE. Selections were carried out as previously described<sup>30</sup>. Antibodies were screened by ELISA for binding to human, cyno and murine ERFE. Cross-reactive binders were then assessed in a C2C12 cell line containing a BMP response element reporter fusion for their ability to interfere with BMP6 signalling. Antibodies capable of interfering with BMP6 signalling were selected for further characterization and used in Homogeneous Time Resolved Fluorescence (HTRF) assays in Fig 1B. A mouse hybridoma approach was also taken to generate anti-ERFE antibodies as described previously<sup>22</sup>; details are in Supplementary Information.

#### **Antibody production**

Transient HEK293 cells expressing anti-ERFE were cultured in FreeStyle™ 293 medium or Expi293™ medium (ThermoFisher, Waltham, MA). These cells were pre-seeded in a wave bioreactor at a cell density of  $1.25 \times 10^6$  cells/ml and transfected with polyethylenimine (Polysciences, Warrington, PA). The wave bioreactors were incubated at 37 °C with a rocking rate of 20 rpm for 120 h before harvest. The conditioned media was centrifuged using a Sorvall™ BIOS 16 Bioprocessing Centrifuge (Thermo Fisher Scientific) and filtered with a 0.22 µm filter device prior to purification. The clarified conditioned media was loaded onto a 5 ml MabSelect SuRe column (GE Life Sciences, Marlborough, MA) equilibrated with PBS, pH 7.2. The column was washed with 10 column volumes of PBS, pH 7.2 before the protein was step eluted using a low pH buffer. The protein was immediately loaded onto a 320 ml Superdex 200 size exclusion column (GE Life Sciences, Marlborough, MA) equilibrated in PBS, pH 7.2. Peak fractions were pooled and filtered through a 0.2µm Polyethersulfone (PES) filter.

#### **Luciferase assay**

C2C12 mouse myoblast cells were transfected with a pTal-Luc reporter plasmid in which a synthetic BMP-response element (BRE) was inserted into the NheI site as previously described<sup>31</sup>. Cells were cultured in Low Bicarbonate DMEM supplemented with 4 mM L-glutamine; 4.5 g/L glucose, 100ug/ml of Pen/Strep; 10% fetal bovine serum (FBS). Cells were plated in a 96 well plate (10 000 cells per well) and treated 24h later in 1% FBS media containing BMP (2nM) alone or in combination with a gradient of mouse ERFE concentrations (4-fold dilutions from 0.5µM) with two replicates per condition. Luminescence was measured 24h after treatment using the britelite Plus Reporter Gene

Assey System (PerkinElmer) and an EnVision Plate Reader (PerkinElmer) following the manufacturer's instructions.

### **Surface plasmon resonance**

The binding affinities of recombinant human (rh) BMP2 (R&D 355-BM/CF), rhBMP4 (R&D 314-BP/CF) and rhBMP6 (R&D 507-BP/CF) to human ERFE were determined using a BIAcore T200 instrument (GE Healthcare) at 15°C with a collection rate of 10 Hz. The running and sample buffer was 10 mM HEPES pH 7.4, 0.3 M NaCl, 3 mM EDTA, 0.05% P-20. Human ERFE was immobilized onto different flow cells of a CM4 sensorchip (GE Healthcare, BR100534) using the Amine Coupling Kit (GE Healthcare, BR-1006-33) according to the manufacturer's protocol. The immobilization level of human ERFE was 256 resonance units (RU). A two-fold dilution series of rhBMP2, rhBMP4 and rhBMP6 and Growth differentiation factor-15 (GDF15) with concentrations ranging from 50 nM to 3.13 nM was injected over the sensor surface for 30 seconds at 100 µl/min. The dissociation was monitored for 300 seconds and the surface was regenerated with 10 mM Glycine pH 1.5. Apparent binding affinities and rate constants were determined by fitting the resulting sensorgram data to a 1:1 Langmuir model in BIAcore T200 Evaluation software version 2.0 (GE Healthcare).

### **Cell culture and treatments**

Huh7 cells were cultured in Dulbecco's Modified Eagle's Medium – High Glucose (Sigma), supplemented with 10% Fetal Bovine Serum (Sigma), 1% Penicillin-Streptomycin (Sigma) and 1% L-Glutamine (Sigma) and maintained at 37°C, 5% CO<sub>2</sub>. Cells were plated 24h before treatments in 24-well cell culture plates. At the time of treatment, cells were washed with PBS and fresh media was added. Cells were treated with human ERFE (F1-F5 subunits, 1µg/ml), or full length mouse ERFE (200ng/ml) in combination with anti-ERFE antibodies (10µg/ml), and analysed 24h after treatments. In both cases non-ERFE treated cells (saline) was used as control. Each treatment was performed using three replicates.

### **Homogeneous Time Resolved Fluorescence**

A competition HTRF assay<sup>32,33</sup> was established in order to assess whether BMPs could compete with neutralising anti-ERFE antibodies for binding to the same/overlapping epitope on recombinant ERFE protein, and was carried out as previously described<sup>22</sup>. See also Supplementary Information.

**Methods for ELISA, RNA isolation, cDNA synthesis and qRT-PCR, tissue non-heme iron measurement, blood parameters, serum iron and transferrin saturation analysis are in Supplementary Information.**

### **Statistical analysis**

Statistical analyses were performed using Prism 7 (GraphPad Software). Statistical significance was assessed using Student's t-test, Mann-Whitney U-test or one-way ANOVA followed by Tukey test for multiple comparisons.

## Results

### ERFE binds to BMP2, BMP4 and BMP6 with different affinities

Previous work from our group described that ERFE inhibits BMP6, thus decreasing hepcidin expression<sup>24</sup>. To further characterize this interaction we performed surface plasmon resonance using the BIAcore platform, and compared ERFE binding to BMP2, BMP4, BMP6 and GDF15 (Figure 1A, B). Analysis demonstrated a high affinity protein-protein interaction between ERFE and BMP6 (apparent  $K_D$  1.17nM), consistent with our hypothesis that ERFE acts as a ligand trap for BMP6. Interestingly, we also observed that ERFE binds BMP2 and BMP4, although with lower affinity than BMP6 (16.15nM and 41.10nM). This observation was supported by Homogeneous Time Resolved Fluorescence (HTRF) data indicating a reduced ability of BMP2 and BMP4 (compared to BMP6) to displace a bound neutralising antibody from human ERFE (Figure 1C). No binding was detected between ERFE and GDF15, a TGF- $\beta$  family protein previously proposed to suppress hepcidin. These data demonstrate that ERFE directly binds BMP6, the main ligand involved in hepcidin regulation in response to iron, but can also bind BMP2 and BMP4.

### The N-terminal domain of ERFE is sufficient to suppress hepcidin

The structure of ERFE shares characteristics with other members of the C1q/ TNF-related protein (CTRP) family: a signal peptide, an N-terminal domain containing a collagen-like domain (G-X-Y), and a globular domain homologous to complement protein C1q (Figure 2A). The N-terminal domain is less conserved than the C1q-like domain both between mouse and human orthologs (71% identity overall, 84% within C1q-like region) and also within human CTRP family as a whole<sup>11</sup>. Computational analysis of the human ERFE amino acid sequence using ProP1.0 software predicted two furin cleavage sites: RARR at position 42 and RLRR at position 212. To understand which ERFE domain(s) are necessary for ERFE activity, we designed and expressed ERFE subunits based on the predicted furin cleavage sites, and tested these in human hepatoma cells (Huh7). Subunits containing most of the N-terminal domain (F2, F4) caused hepcidin suppression to a similar extent as subunits containing that region plus the globular C1q (F3) and the full length protein, indicating that the N-terminal domain is sufficient for ERFE activity (Figure 2B). In the absence of the N-terminus, subunits containing the signal peptide (F1) or most of the globular C1q (F5) domain did not affect hepcidin expression. Consistent with this, a peptide containing the whole C1q domain also failed to suppress hepcidin (Figure S1) indicating that this portion of the protein is not required for hepcidin suppressive activity *in vitro*.

Previous data from our group has shown that full-length ERFE directly suppresses hepcidin and BMP target genes in mice 3 hours after an intravenous injection with recombinant protein. To corroborate our *in vitro* data on functionality of ERFE subunits, we treated mice with F2 ERFE, containing the signal peptide and the N-terminal domain but not the globular C1q domain. Analysis at 3 hours after treatment showed suppression of *Hamp* and other BMP-target genes (*Id1*, *Id2*, *Atoh8*, *Smad7*), with no suppression of *Bmp2* or *Bmp6* (Figure 2C). These data confirm our previous findings that ERFE suppresses hepcidin and BMP signalling *in vivo*, and demonstrate that the N-terminal domain is sufficient for ERFE activity.

### **Neutralizing Anti-ERFE antibodies bind to the N-terminal region of ERFE**

Abnormally high circulating ERFE levels are associated with increased severity of  $\beta$ -thalassemia<sup>26</sup>, causing persistent hepcidin suppression, which leads to iron accumulation. To neutralize excess ERFE, we developed anti-ERFE antibodies by immunizing ERFE KO mice with full-length protein. After antibody purification, we tested the binding capacity of the antibodies to different regions of ERFE by ELISA and identified antibodies that exclusively bind to the N-terminal domain (mAbs 15.1 and 20.1) or globular C1q domain (mAb 28.1, Figure 3A). Homogenous time-resolved fluorescence (HTRF) analysis showed that binding of an anti-N-terminus antibody to full-length ERFE is not strongly inhibited by anti-C-terminus antibody and that binding of anti-N-terminus antibody to ERFE, but not binding of anti-C-terminus antibody, is potently and dose-dependently inhibited by BMP6 (Figure 3B), showing that the BMP6 binding site is fully or partially contained within the N-terminus. This is consistent with a proposed mechanism for ERFE action in which the N-terminal domain of ERFE binds BMP6 and acts as a ligand trap to suppress BMP/SMAD signalling and hepcidin expression.

We next tested the capacity of the antibodies to neutralize ERFE *in vitro*. As expected, Huh7 cells treated with full-length recombinant mouse ERFE suppressed hepcidin (Figure 3C). When the same conditions were used in the presence of an anti-ERFE monoclonal antibody (15.1 or 20.1), hepcidin suppression was absent (15.1) or severely blunted (20.1), indicating that both antibodies targeting the N-terminal domain neutralize ERFE.

### **Antibodies binding ERFE N-terminal domain block hepcidin suppression in EPO-treated mice**

ERFE expression and production in erythroblasts is stimulated by erythropoietin (EPO); under basal physiological conditions the mRNA is lowly expressed by those cells (and there are fewer such cells). To test our antibodies in a model of increased erythropoiesis (leading to increased ERFE), we injected WT mice with 200 units of EPO plus an antibody control (IgG2A) or one of the two neutralizing antibodies described above and analysed the mice 18h after treatment. In the presence of control IgG2A, EPO suppressed hepcidin (Figure 4A) leading to lower circulating hepcidin protein (Figure 4B). Simultaneous injection of EPO and anti-ERFE antibody prevented hepcidin suppression and rescued circulating hepcidin to the levels observed in non-EPO treated mice. To test the functional impact of ERFE neutralization on erythropoietic output, we increased the dose to 3 EPO injections on three consecutive days, with simultaneous injection of anti-ERFE antibody on days 1 and 3, and analysis of blood parameters on day 4 (Figure S2). In these conditions, we observed a moderate (15.1) or a significant elevation (20.1) in *Hamp* expression compared to EPO treated mice (Figure S2A), decreased serum iron and unchanged liver iron (Figure S2B). Various blood parameters were increased by EPO treatment (Hemoglobin, Hematocrit, Mean Corpuscular Volume and Red Cell Distribution Width). These increases were partially prevented by treatment with anti-ERFE (Figure S2C). Thus, inhibition of ERFE impacts hepcidin and erythropoiesis output in response to EPO.

### **Anti-ERFE antibodies decrease iron levels and alter blood parameters in thalassemic mice**

To assess the capacity of anti-ERFE antibodies as a potential therapeutic to prevent iron overload in  $\beta$ -thalassemia, we initially tested both anti-N-terminus Erfe antibodies in Hbb(th3/+) mice, a model of thalassemia intermedia. Mice were treated with anti-ERFE or IgG2A control bi-weekly for 4 weeks,



starting at 4 weeks of age. During this period, these mice accumulate iron associated with suppressed hepcidin and increased ERFE expression<sup>25</sup>, characteristics observed in human patients. Compared to WT mice, IgG2A-treated thalassemic mice had lower serum iron and transferrin saturation (Figure 5B), and increased iron accumulation in the liver and spleen (Figure 5C). Treatment with both anti-ERFE antibodies caused a further decrease in serum iron and antibody 15.1 partially prevented iron accumulation in the liver. However, serum hepcidin levels were not significantly different between groups (Figure 5A). Thus, the lower levels of serum and liver iron in anti-ERFE-treated mice were not paralleled with decreased hepcidin, indicating that hepcidin might be relatively increased by anti-ERFE treatment. Concurrently, treatment with anti-ERFE antibodies increased the number of red blood cells, hemoglobin concentration and haematocrit, while decreasing the number of reticulocytes and the red cell distribution width (Figure 5E). To further assess the effects of an anti-ERFE antibody, we increased the dosing period to 8 weeks, which led to more pronounced effects: anti-ERFE 15.1 treatment caused an increase in hepatic hepcidin mRNA expression, a decrease in liver iron and so an increased Hamp to liver iron content (LIC) ratio (Fig 6A-C). Serum iron was decreased, spleen iron concentration was not significantly different but a reduction in spleen/body ratio was observed (Fig 6D-F). This indicates an amelioration of splenomegaly, a major feature of  $\beta$ -thalassemia that is recapitulated in Hbb(th3/+) mice. Increased red blood cells, hemoglobin and haematocrit, and fewer reticulocytes, were also evident (Figure 6G). Overall, anti-ERFE antibodies decreased iron accumulation in thalassaemic mice and improved anemia.

## Discussion

The existence of an erythroid regulator that increases iron availability in response to erythropoietic demand has long been hypothesized<sup>34</sup>, and the discovery of ERFE provided a strong candidate to fill that role<sup>21</sup>. Increasing hepcidin activity is a therapeutic goal for iron loading anemias such as  $\beta$ -thalassemia, and inhibiting ERFE activity is one potential method of achieving this (among others<sup>27,35,36,37,38</sup>); antibodies that specifically bind ERFE were recently described (<https://patents.google.com/patent/WO2018027184A1/en>). We generated ERFE-neutralizing antibodies that rescue ERFE-mediated hepcidin suppression both *in vitro* (Figure 3C) and in mice injected with EPO (Figures 4 and S2), and which decreased serum and liver iron in thalassemic mice (Figure 5 and 6). Liver iron in anti-ERFE-treated Hbb(th3/+) mice was not reduced to the levels observed in WT mice, this may be due to iron accumulation prior to administration of anti-ERFE, and/or because the increase in hepcidin mediated by anti-ERFE is not sufficient to completely inhibit dietary absorption. Even though the Hbb(th3/+) mice recapitulate many of the features of the human disease (low hemoglobin, increase in reticulocyte numbers, aberrant erythrocyte morphology and tissue iron overload<sup>39,40</sup>) mice normalize hepcidin expression after 12 weeks of age, in contrast to human patients who present chronic hepcidin suppression throughout adulthood<sup>41-43</sup>. For this reason, we hypothesize that neutralizing ERFE in human  $\beta$ -thalassemia might have a more pronounced impact than in mice. Concurrent with the decrease in iron, we observed an amelioration of ineffective erythropoiesis with an increase in the number of red blood cells, hemoglobin, and haematocrit with decreased number of reticulocytes, mean corpuscular volume and cell distribution width. Based on previous works by others, we can speculate that iron restriction may induce a

reduction in heme synthesis to lower the amount of alpha-globin thus equilibrating  $\alpha$  and  $\beta$  chains, and potentially reducing reactive oxygen species<sup>44,45</sup>.

We have previously shown that ERFE inhibits BMP6 and suppresses hepcidin expression<sup>24</sup>. Here we show using Biacore that the direct BMP6-ERFE interaction is of high affinity ( $\sim 1.17$  nM), which contrasts with the estimated lower affinity of a Tfr2-BMP interaction ( $\sim 400$  nM)<sup>46</sup>. The development of anti-ERFE antibodies was also used as a tool to further investigate the ERFE mechanism of action. Using HTRF as a competition assay between anti-ERFE mAbs and BMP6 we show that BMP6 binds to a region of ERFE contained within the N-terminal domain (Figure 3B). Consistent with this notion, the ERFE N-terminal domain was sufficient to suppress hepcidin expression both *in vitro* and in mice (Figure 2). Therefore, we demonstrate that ERFE-mediated hepcidin suppression is caused by the N-terminal domain binding to BMP6. The N-terminal region is generally less conserved than the C1q-like domain (which mediates multimerization) and may confer specific activities upon individual CTRP family members.

Besides BMP6, we have previously shown that ERFE binds BMP5 and BMP7, which are closely related to BMP6 but are not currently regarded as regulators of iron metabolism *in vivo*. Although BMP7 does not have a described physiological role in iron homeostasis, the ability of ERFE to bind this BMP may be relevant in situations in which lack of BMP6 is compensated by an increase in BMP7 expression<sup>47</sup>. Here, we expanded our analysis to BMP2 and BMP4. BMP2 regulates liver hepcidin expression independently of BMP6<sup>20</sup> and BMP4 is structurally related but its physiological relevance with respect to hepcidin regulation is not yet clear. Interestingly, we observed that ERFE does bind these two BMPs, although with significantly lower affinity than binding to BMP6 (Figure 1). ERFE does not strongly impair the ability of BMP2 to stimulate hepcidin synthesis *in vitro*<sup>24</sup>, but could conceivably influence BMP2 activity *in vivo* in the absence of BMP6. We recently showed that ERFE can inhibit BMP2 signalling in subcutaneous abdominal preadipocytes<sup>48</sup>. Furthermore, ERFE may modulate bone metabolism in  $\beta$ -thalassemia by a mechanism that may involve BMPs<sup>49</sup>; further work is needed to investigate the role of ERFE beyond hepcidin regulation. The relative inability of ERFE to functionally impair BMP2-induced hepcidin induction compared to BMP6, despite ERFE binding BMP2 and influencing BMP signalling in non-hepatocyte cell types, may be related to structural variation in different BMPs<sup>17</sup> and/or differences in how BMP-ERFE complexes interact with available receptor / co-receptor combinations on distinct cell types. Structural analysis of ERFE and BMPs and their receptors is required to further investigate this issue. GDF15, previously proposed to control hepcidin expression in response to erythropoiesis<sup>50</sup>, did not bind ERFE, indicating that not all members of the TGF- $\beta$  superfamily are affected by ERFE.

In summary, by identifying the active region of ERFE and the binding affinity to different BMPs we increased our understanding of ERFE mechanism of action. We describe the development of ERFE N-terminus –targeted antibodies that neutralize ERFE-mediated hepcidin suppression and ameliorate the iron-loaded phenotype in a mouse model of  $\beta$ -thalassemia, indicating their potential therapeutic utility to treat this disease.

## **Acknowledgments**

The authors would like to thank Elizabeth DiBlasio Smith and Chris Corcoran for contributions to protein purification; Darren Ferguson, Caryl Meade and Ashley Schwab for contributions to antibody production; Jonathon Merrill, Jordan Tanner and Roo Bhasin for contributions to the techniques involving mice, and Sarah Gooding for useful advice. This work was funded by a Pfizer-Sponsored Rare Disease Consortium Award, the Medical Research Council UK (MRC Human Immunology Unit core funding MC\_UU\_12010/10 to HD). SJD is a Jenner Investigator, a Lister Institute Research Prize Fellow and a Wellcome Trust Senior Fellow (106917/Z/15/Z).

## **Data sharing**

For original data, please contact the corresponding author.

## **Authorship Contributions**

JA, NF, KM, SB, AEA, SRP, DDP, JEM, EL, OC, ML, SJD, RJ and HD designed research; JA, NF, KM, AS, MST, DQ, SB, PJJ, JNF, AEA and SRP performed research; JA, NF, KM, SB, AS, MST, PJJ, JNF, AEA and SRP collected data; JA, NF, KM, AS, SB, OC, ML, SJD, RJ and HD analyzed and interpreted data; JA and NF performed statistical analysis; JA, NF, RJ and HD wrote the manuscript.

## **Conflict of Interest Disclosures**

This work was supported in part by funding from Pfizer to JA, KM, DQ, SJD and HD. NF, AS, SB, EL, MST, DDP, OC, ML, JEM and RJ are employed by Pfizer. NF, OC, RJ, JA, KM, SJD, and HD are named inventors on a patent application currently under evaluation. The remaining authors declare no competing financial interests.

## Figure legends

**Figure 1: ERFE binds to BMP2, BMP4 and BMP6 with different affinities. (A)** Binding kinetics of ERFE to BMP2, BMP4, BMP6 and GDF15 assessed by Surface Plasmon Resonance (BIAcore). No binding was observed for GDF15. Full length human ERFE was immobilized in a CM4 chip. BMPs/ GDF15 were tested at different concentration (3.1nM – 50nM) for binding to immobilized ERFE and assayed for up to 60 seconds (two replicates per condition). RU: Resonance units. Apparent kD was calculated for binding of BMP2, BMP4 and BMP6 to ERFE (assuming 1:1 binding interaction). **(B)** Apparent KD of ERFE to BMP2, BMP4 and BMP6. **(C)** Homogeneous Time Resolved Fluorescence (HTRF) assay for detection of binding competition between BMPs (0.1-400nM) and an anti-ERFE antibody. Unlabelled anti-ERFE antibody (anti-ERFE) and a control IgG antibody were used as positive and negative controls, respectively. Values calculated as  $\% \Delta F = [(F665 \text{ Sample}/F615 \text{ Sample}) - (F665 \text{ Control}/F615 \text{ Control})] \times 100$ . Data plotted as “% Control” representing the background fluorescence energy transfer in wells containing 1:1000 of each labelled antibody, in assay buffer, alone.

**Figure 2: The N-terminal domain of ERFE is sufficient to suppress hepcidin. (A)** Structure of human ERFE, containing a signal peptide (SP), N-terminal region (NTD) with a collagen-like domain (6 GXY), and a globular C1q domain (gC1Q). The location of the two predicted furin cleavage sites are indicated (RARR and RLRR). ERFE subunits designed and expressed based on predicted furin cleavage sites (F1-5) **(B)** Huh7 cells were treated for 24h with 1µg/ml of ERFE subunits F1-F5, full-length or vehicle and analysed for *HAMP* gene expression **(C)** WT mice were treated intraperitoneally with 100 µg of F2 ERFE or saline and analysed 3h after treatment for liver gene expression of BMP target genes, *Bmp2*, and *Bmp6*. Columns represent mean + standard deviation. n=3 replicates per group (B); n=6 mice per group (C). \*P<0.05; \*\*P <0.01; \*\*\*P<0.001; \*\*\*\*P<0.0001 using Student t test.

**Figure 3: Neutralizing anti-ERFE antibodies bind to the N-terminal region of ERFE. (A)** Anti-ERFE antibodies (15.1, 20.1 and 28.1) were assayed at different concentrations ( $10^{-5}$  –  $10^2$  nM) in ELISA plates coated with full length ERFE, Fur4 (N-terminal domain region) and the globular C1q domain. **(B)** Homogeneous Time Resolved Fluorescence (HTRF) assay for detection of binding competition using cryptate-labelled antiERFE antibodies (20.1 and 28.1) and BMP6 (0.1 – 200nM), and unlabelled antibody as positive control. Values calculated as  $\% \Delta F = [(F665 \text{ Sample}/F615 \text{ Sample}) - (F665 \text{ Control}/F615 \text{ Control})] \times 100$ . Data plotted as “% Control” representing the background fluorescence energy transfer in wells containing 1:1000 of each labelled antibody, in assay buffer, alone; **(C)** Huh7 cells were treated for 24h with 200ng/ml of murine ERFE alone or in combination with 10µg/ml of anti-ERFE antibodies 15.1 and 20.1, and analyzed for *HAMP* gene expression. Bars represent mean +/-standard deviation. n=3 replicates per group; \*\*\*P<0.001; \*\*\*\*P<0.0001 using Student t test.

**Figure 4: Antibodies binding ERFE N-terminal domain block hepcidin suppression in EPO-treated mice.** Eight-week old male WT mice were treated intraperitoneally with 200 units of erythropoietin (EPO) in combination with intravenous injection of an IgG2A antibody control, anti-ERFE 15.1 or anti ERFE 20.1 (or vehicle alone instead of EPO for analysis of baseline values). Mice were euthanized and analysed 18h after treatment for analysis of *Hamp* expression **(A)** and serum hepcidin **(B)**. n= 3

(vehicle), 5-6 (EPO-treated mice). \* $P < 0.05$ ; \*\*\* $P < 0.001$ ; \*\*\*\* $P < 0.0001$  using Student t test. \* $P < 0.05$ ; \*\* $P < 0.01$ ; \*\*\* $P < 0.001$ ; \*\*\*\* $P < 0.0001$  using Student t test.

**Figure 5: Antibodies targeting the N-terminal domain of ERFE decrease iron levels and alter blood parameters in thalassemic mice.** Four-week old male Hbb(th3/+) mice were treated intravenously with 5mg/kg of IgG2A control antibody, anti-ERFE 15.1 or anti-ERFE 20.1, twice a week for four weeks. IgG2A-treated wildtype mice were used as control for basal levels. After 4 weeks of treatment mice were euthanized for analysis of serum hepcidin **(A)**, serum iron and transferrin saturation **(B)**, liver and spleen non-heme iron **(C)**, spleen to body weight ratio **(D)** and blood parameters **(E)**. \* $P < 0.05$ ; \*\* $P < 0.01$ ; \*\*\* $P < 0.001$ ; \*\*\*\* $P < 0.0001$  using one-way ANOVA followed by Tukey's test for differences between IgG2A-treated Hbb(th3/+) and antiERFE-treated mice. # $P < 0.05$ , ##### $P < 0.0001$  using one-way ANOVA followed by Tukey's test for differences between wildtype and Hbb(th3/+) mice. RBC: Red Blood Cells; HGB: Hemoglobin; HCT: Hematocrit; MCV: Mean Corpuscular Volume; RDW: Red Cell Distribution Width. n=5-8 mice per group.

**Figure 6: Antibodies targeting the N-terminal domain of ERFE increase hepcidin expression and ameliorate anemia in thalassemic mice.** Four-weeks old male Hbb(th3/+) mice were treated intravenously with 5mg/kg of IgG2A control antibody or anti-ERFE 15.1, twice a week for eight weeks. After 8 weeks of treatment mice were euthanized for analysis of liver hepcidin mRNA expression **(A)**, liver non-heme iron **(B)**, *Hamp* to liver non-heme iron content (LIC) ratio **(C)**, serum iron **(D)**, spleen non-heme iron **(E)**, spleen to body weight **(F)**, and blood parameters **(G)**. \* $P < 0.05$ ; \*\* $P < 0.01$ ; \*\*\* $P < 0.001$  using the Mann-Whitney test. LIC: liver iron content; RBC: Red Blood Cells; HGB: Hemoglobin; HCT: Hematocrit; n=6 (IgG2A group); n=9 (15.1 group).

## References

1. Rachmilewitz EA, Giardina PJ. How I treat thalassemia. *Blood*. 2011;118(13):3479-3488.
2. Taher AT, Weatherall DJ, Cappellini MD. Thalassaemia. *Lancet*. 2018;391(10116):155-167.
3. Flint J, Harding RM, Boyce AJ, Clegg JB. The population genetics of the haemoglobinopathies. *Baillieres Clin Haematol*. 1998;11(1):1-51.
4. Musallam KM, Taher AT, Rachmilewitz EA. beta-thalassemia intermedia: a clinical perspective. *Cold Spring Harb Perspect Med*. 2012;2(7):a013482.
5. Tantiworawit A, Charoenkwan P, Hantrakool S, Choeprasert W, Sivasomboon C, Sanguansermisri T. Iron overload in non-transfusion-dependent thalassemia: association with genotype and clinical risk factors. *Int J Hematol*. 2016;103(6):643-648.
6. Musallam KM, Motta I, Salvatori M, et al. Longitudinal changes in serum ferritin levels correlate with measures of hepatic stiffness in transfusion-independent patients with beta-thalassemia intermedia. *Blood Cells Mol Dis*. 2012;49(3-4):136-139.
7. Restivo Pantalone G, Renda D, Valenza F, et al. Hepatocellular carcinoma in patients with thalassaemia syndromes: clinical characteristics and outcome in a long term single centre experience. *Br J Haematol*. 2010;150(2):245-247.
8. Mancuso A. Hepatocellular carcinoma in thalassemia: A critical review. *World J Hepatol*. 2010;2(5):171-174.
9. Musallam KM, Cappellini MD, Wood JC, et al. Elevated liver iron concentration is a marker of increased morbidity in patients with beta thalassemia intermedia. *Haematologica*. 2011;96(11):1605-1612.
10. Saliba AN, Harb AR, Taher AT. Iron chelation therapy in transfusion-dependent thalassemia patients: current strategies and future directions. *J Blood Med*. 2015;6:197-209.
11. Pasricha SR, McHugh K, Drakesmith H. Regulation of Hepcidin by Erythropoiesis: The Story So Far. *Annu Rev Nutr*. 2016;36:417-434.
12. Nemeth E, Tuttle MS, Powelson J, et al. Hepcidin regulates cellular iron efflux by binding to ferroportin and inducing its internalization. *Science*. 2004;306(5704):2090-2093.
13. Aschemeyer S, Qiao B, Stefanova D, et al. Structure-function analysis of ferroportin defines the binding site and an alternative mechanism of action of hepcidin. *Blood*. 2017.
14. Gardenghi S, Marongiu MF, Ramos P, et al. Ineffective erythropoiesis in beta-thalassemia is characterized by increased iron absorption mediated by down-regulation of hepcidin and up-regulation of ferroportin. *Blood*. 2007;109(11):5027-5035.
15. Andriopoulos B, Jr., Corradini E, Xia Y, et al. BMP6 is a key endogenous regulator of hepcidin expression and iron metabolism. *Nat Genet*. 2009;41(4):482-487.
16. Meynard D, Kautz L, Darnaud V, Canonne-Hergaux F, Coppin H, Roth MP. Lack of the bone morphogenetic protein BMP6 induces massive iron overload. *Nat Genet*. 2009;41(4):478-481.
17. Yadin D, Knaus P, Mueller TD. Structural insights into BMP receptors: Specificity, activation and inhibition. *Cytokine Growth Factor Rev*. 2016;27:13-34.
18. Lim PJ, Duarte TL, Arezes J, et al. Nrf2 controls iron homeostasis in haemochromatosis and thalassaemia via Bmp6 and hepcidin. *Nat Metab*. 2019;1(5):519-531.
19. Kautz L, Meynard D, Monnier A, et al. Iron regulates phosphorylation of Smad1/5/8 and gene expression of Bmp6, Smad7, Id1, and Atoh8 in the mouse liver. *Blood*. 2008;112(4):1503-1509.
20. Canali S, Wang CY, Zumbrennen-Bullough KB, Bayer A, Babitt JL. Bone morphogenetic protein 2 controls iron homeostasis in mice independent of Bmp6. *Am J Hematol*. 2017;92(11):1204-1213.
21. Kautz L, Jung G, Valore EV, Rivella S, Nemeth E, Ganz T. Identification of erythroferrone as an erythroid regulator of iron metabolism. *Nat Genet*. 2014;46(7):678-684.
22. Wang CY, Core AB, Canali S, et al. Smad1/5 is required for erythropoietin-mediated suppression of hepcidin in mice. *Blood*. 2017;130(1):73-83.

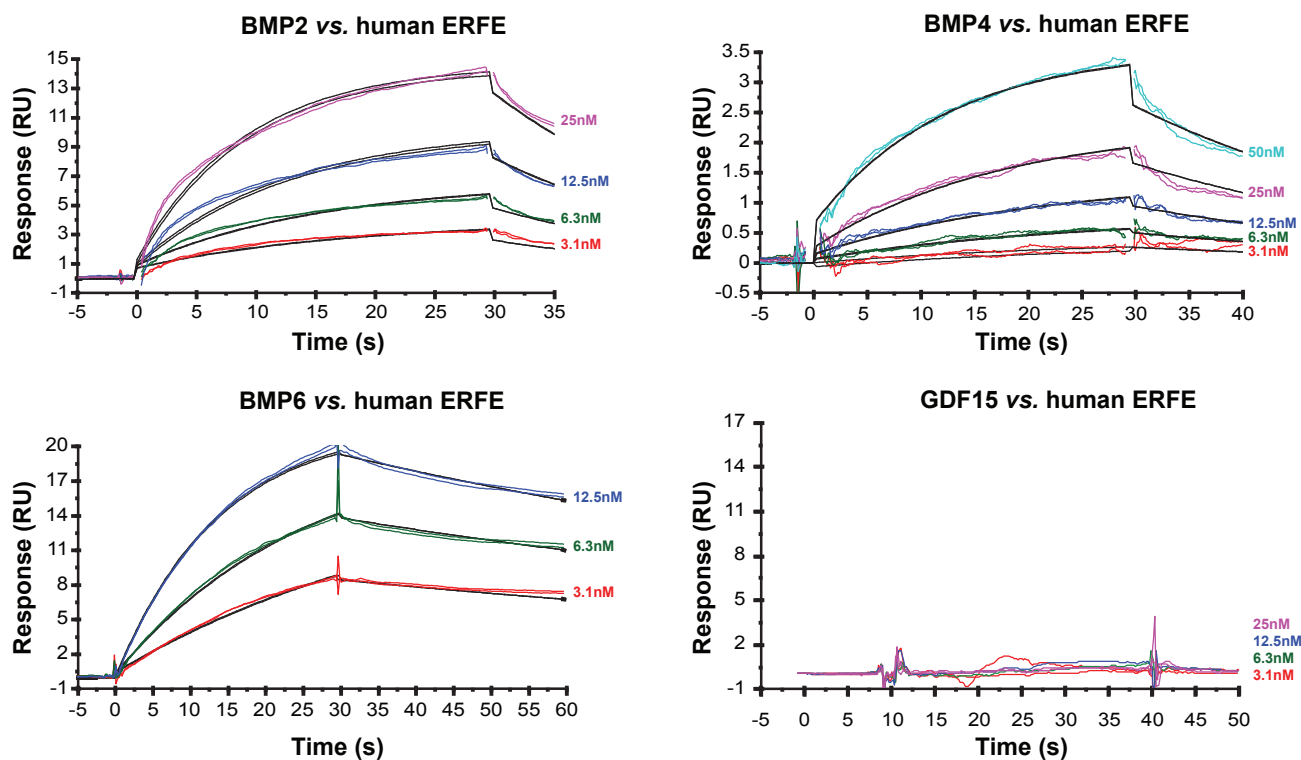
23. Aschemeyer S, Gabayan V, Ganz T, Nemeth E, Kautz L. Erythroferrone and matriptase-2 independently regulate hepcidin expression. *Am J Hematol*. 2017.
24. Arezes J, Foy N, McHugh K, et al. Erythroferrone inhibits the induction of hepcidin by BMP6. *Blood*. 2018;132(14):1473-1477.
25. Kautz L, Jung G, Du X, et al. Erythroferrone contributes to hepcidin suppression and iron overload in a mouse model of beta-thalassemia. *Blood*. 2015;126(17):2031-2037.
26. Ganz T, Jung G, Naeim A, et al. Immunoassay for human serum erythroferrone. *Blood*. 2017;130(10):1243-1246.
27. Casu C, Oikonomidou PR, Chen H, et al. Minihepcidin peptides as disease modifiers in mice affected by beta-thalassemia and polycythemia vera. *Blood*. 2016;128(2):265-276.
28. Casu C, Chessa R, Liu A, et al. Minihepcidins improve ineffective erythropoiesis and splenomegaly in a new mouse model of adult beta-thalassemia major. *Haematologica*. 2019.
29. Ishino T, Wang M, Mosyak L, et al. Engineering a monomeric Fc domain modality by N-glycosylation for the half-life extension of biotherapeutics. *J Biol Chem*. 2013;288(23):16529-16537.
30. Finlay WJ, Bloom L, Cunningham O. Optimized generation of high-affinity, high-specificity single-chain Fv antibodies from multiantigen immunized chickens. *Methods Mol Biol*. 2011;681:383-401.
31. Korchynskyi O, ten Dijke P. Identification and functional characterization of distinct critically important bone morphogenetic protein-specific response elements in the Id1 promoter. *J Biol Chem*. 2002;277(7):4883-4891.
32. Finlay WJ, Cunningham O, Lambert MA, et al. Affinity maturation of a humanized rat antibody for anti-RAGE therapy: comprehensive mutagenesis reveals a high level of mutational plasticity both inside and outside the complementarity-determining regions. *J Mol Biol*. 2009;388(3):541-558.
33. Degorce F, Card A, Soh S, Trinquet E, Knapik GP, Xie B. HTRF: A technology tailored for drug discovery - a review of theoretical aspects and recent applications. *Curr Chem Genomics*. 2009;3:22-
34. Finch C. Regulators of iron balance in humans. *Blood*. 1994;84(6):1697-1702.
35. Rivella S. beta-thalassemias: paradigmatic diseases for scientific discoveries and development of innovative therapies. *Haematologica*. 2015;100(4):418-430.
36. Guo S, Casu C, Gardenghi S, et al. Reducing TMPRSS6 ameliorates hemochromatosis and beta-thalassemia in mice. *J Clin Invest*. 2013;123(4):1531-1541.
37. Schmidt PJ, Toudjarska I, Sendamarai AK, et al. An RNAi therapeutic targeting Tmprss6 decreases iron overload in Hfe(-/-) mice and ameliorates anemia and iron overload in murine beta-thalassemia intermedia. *Blood*. 2013;121(7):1200-1208.
38. Li H, Rybicki AC, Suzuka SM, et al. Transferrin therapy ameliorates disease in beta-thalassemic mice. *Nat Med*. 2010;16(2):177-182.
39. Gardenghi S, Ramos P, Marongiu MF, et al. Hepcidin as a therapeutic tool to limit iron overload and improve anemia in beta-thalassemic mice. *J Clin Invest*. 2010;120(12):4466-4477.
40. Adamsky K, Weizer O, Amariglio N, et al. Decreased hepcidin mRNA expression in thalassemic mice. *Br J Haematol*. 2004;124(1):123-124.
41. Origa R, Galanello R, Ganz T, et al. Liver iron concentrations and urinary hepcidin in beta-thalassemia. *Haematologica*. 2007;92(5):583-588.
42. Kearney SL, Nemeth E, Neufeld EJ, et al. Urinary hepcidin in congenital chronic anemias. *Pediatr Blood Cancer*. 2007;48(1):57-63.
43. Jones E, Pasricha SR, Allen A, et al. Hepcidin is suppressed by erythropoiesis in hemoglobin E beta-thalassemia and beta-thalassemia trait. *Blood*. 2015;125(5):873-880.
44. Camaschella C. Treating iron overload. *N Engl J Med*. 2013;368(24):2325-2327.
45. Gardenghi S, Grady RW, Rivella S. Anemia, ineffective erythropoiesis, and hepcidin: interacting factors in abnormal iron metabolism leading to iron overload in beta-thalassemia. *Hematol Oncol Clin North Am*. 2010;24(6):1089-1107.

46. Rauner M, Baschant U, Roetto A, et al. Transferrin receptor 2 controls bone mass and pathological bone formation via BMP and Wnt signaling. *Nat Metab.* 2019;1(1):111-124.
47. Pauk M, Grgurevic L, Brkljacic J, et al. Exogenous BMP7 corrects plasma iron overload and bone loss in Bmp6<sup>-/-</sup> mice. *Int Orthop.* 2015;39(1):161-172.
48. Denton NF, Eghleilib M, Al-Sharifi S, et al. Bone morphogenetic protein 2 is a depot-specific regulator of human adipogenesis. *Int J Obes (Lond).* 2019.
49. Castro-Mollo M, Ruiz Martinez M, Feola M, et al. Erythroferrone Regulates Bone Remodeling in beta-Thalassemia. *Blood.* 2019;134(Supplement\_1):2.
50. Tanno T, Bhanu NV, Oneal PA, et al. High levels of GDF15 in thalassemia suppress expression of the iron regulatory protein hepcidin. *Nat Med.* 2007;13(9):1096-1101.



# Figure 1

A



B

Analyte	Apparent KD (nM)
BMP2	16.15
BMP4	41.10
BMP6	1.17
GDF15	No binding

C

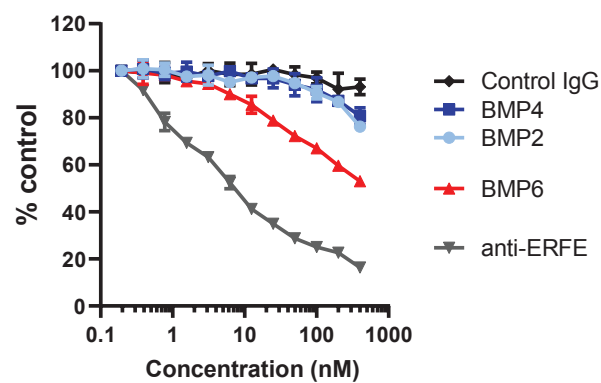
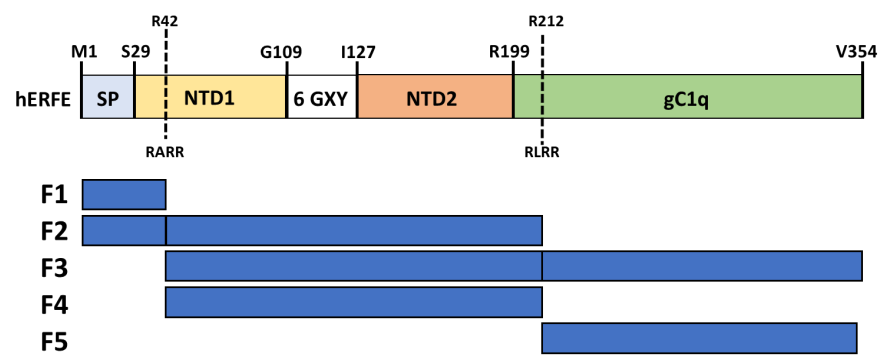
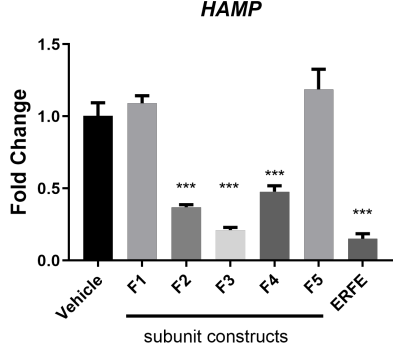


Figure 2

A



B



C

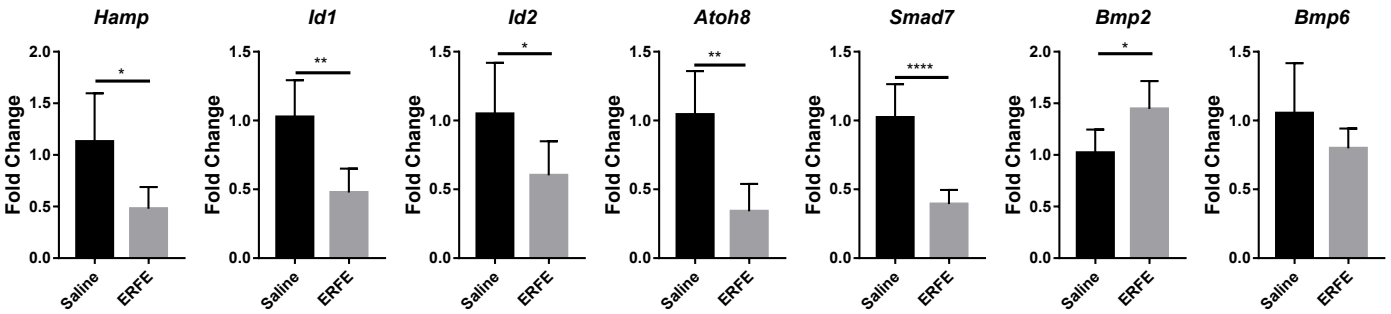


# Figure 3

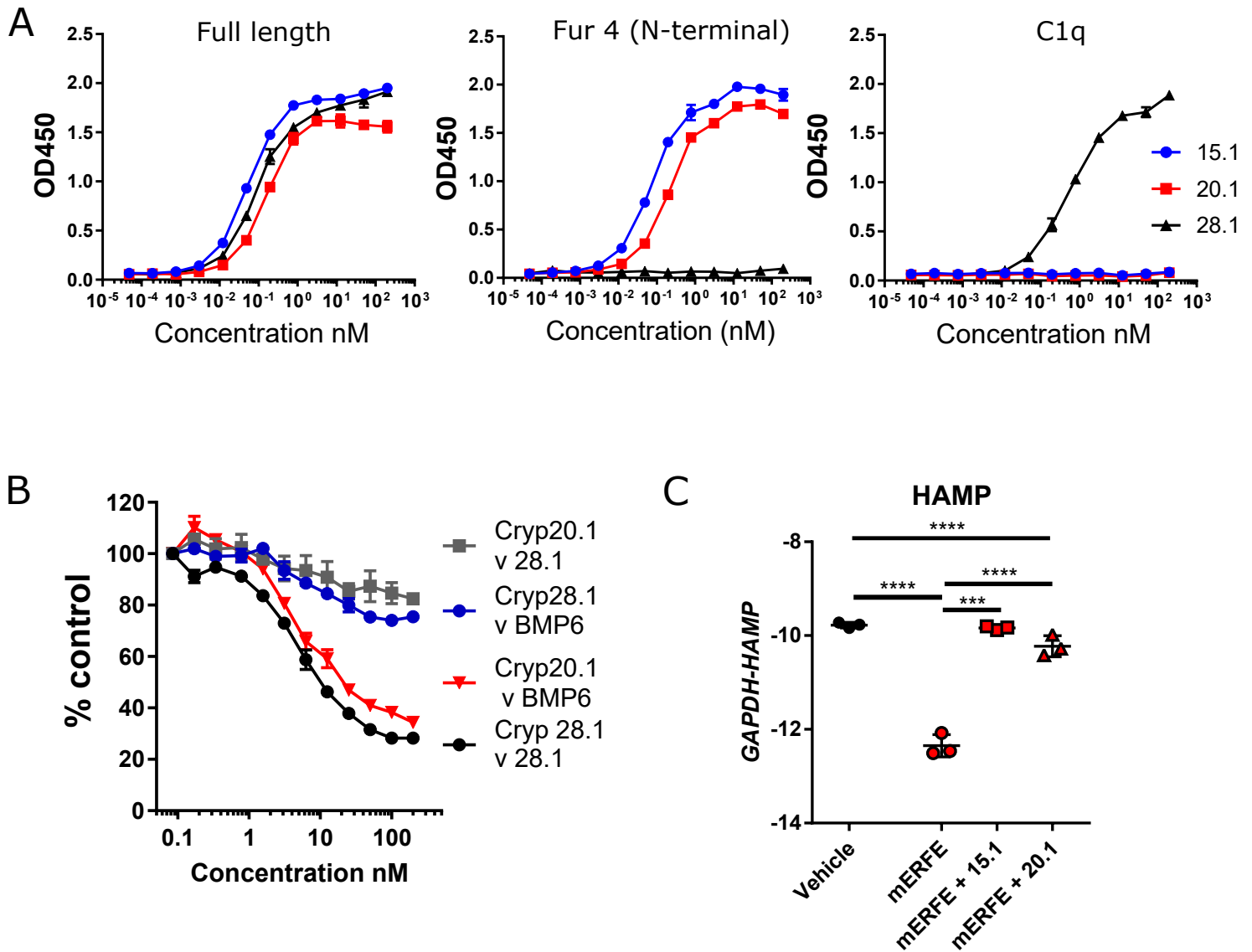


# Figure 4

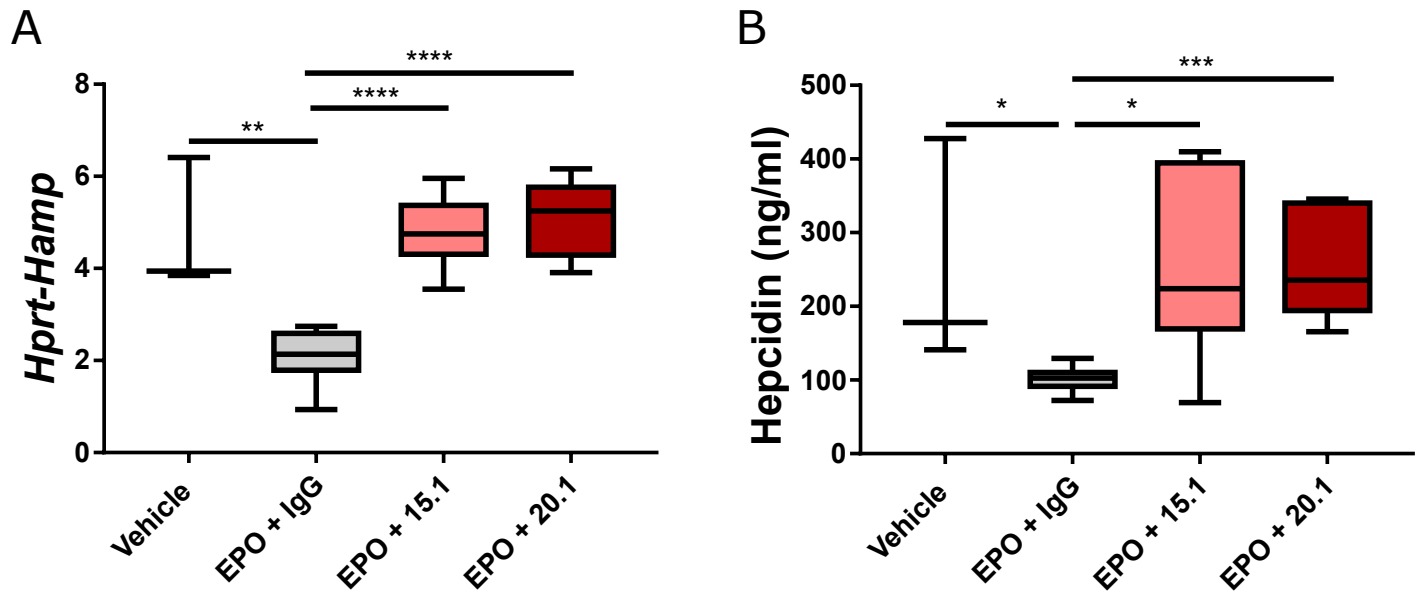


# Figure 5

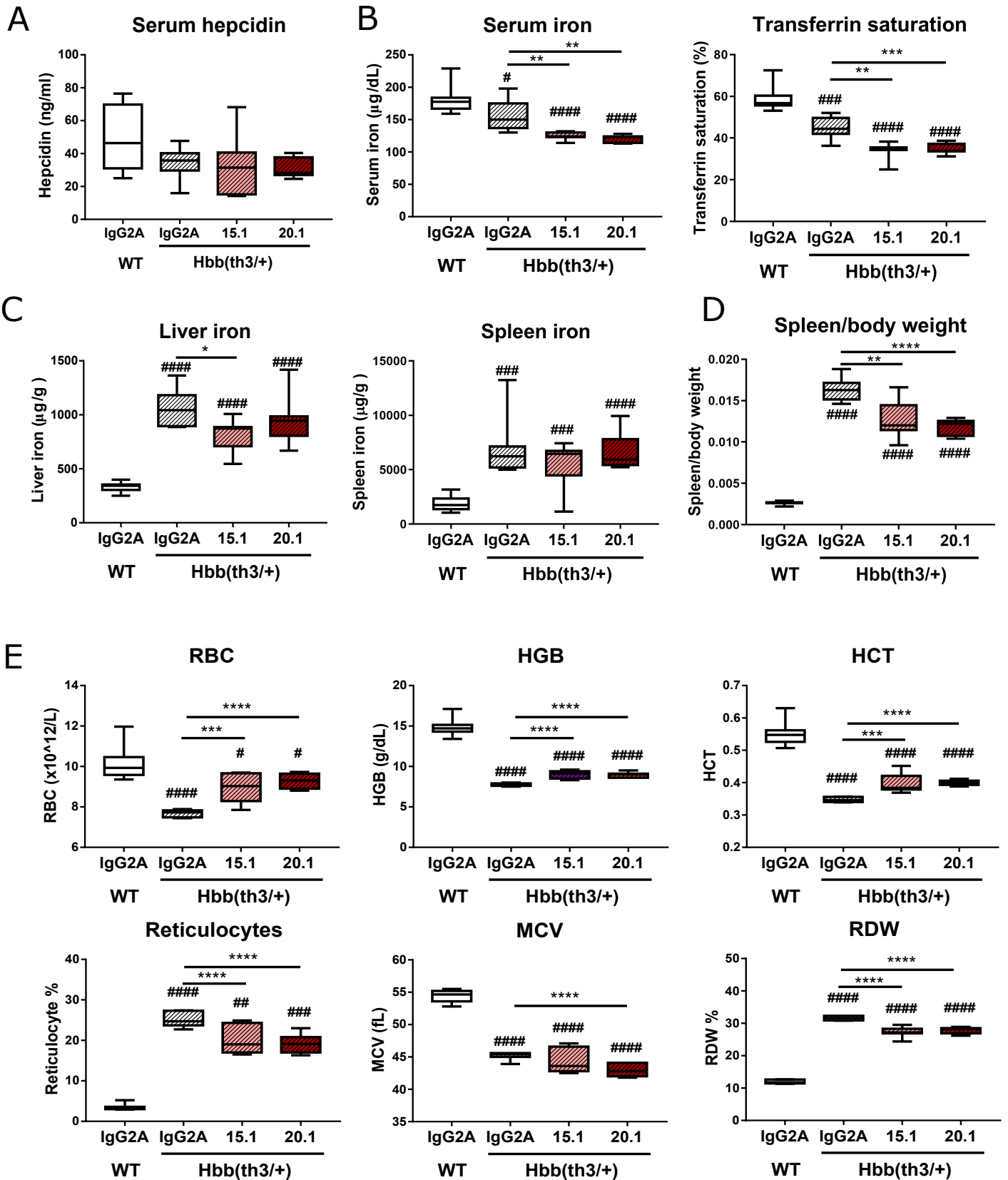
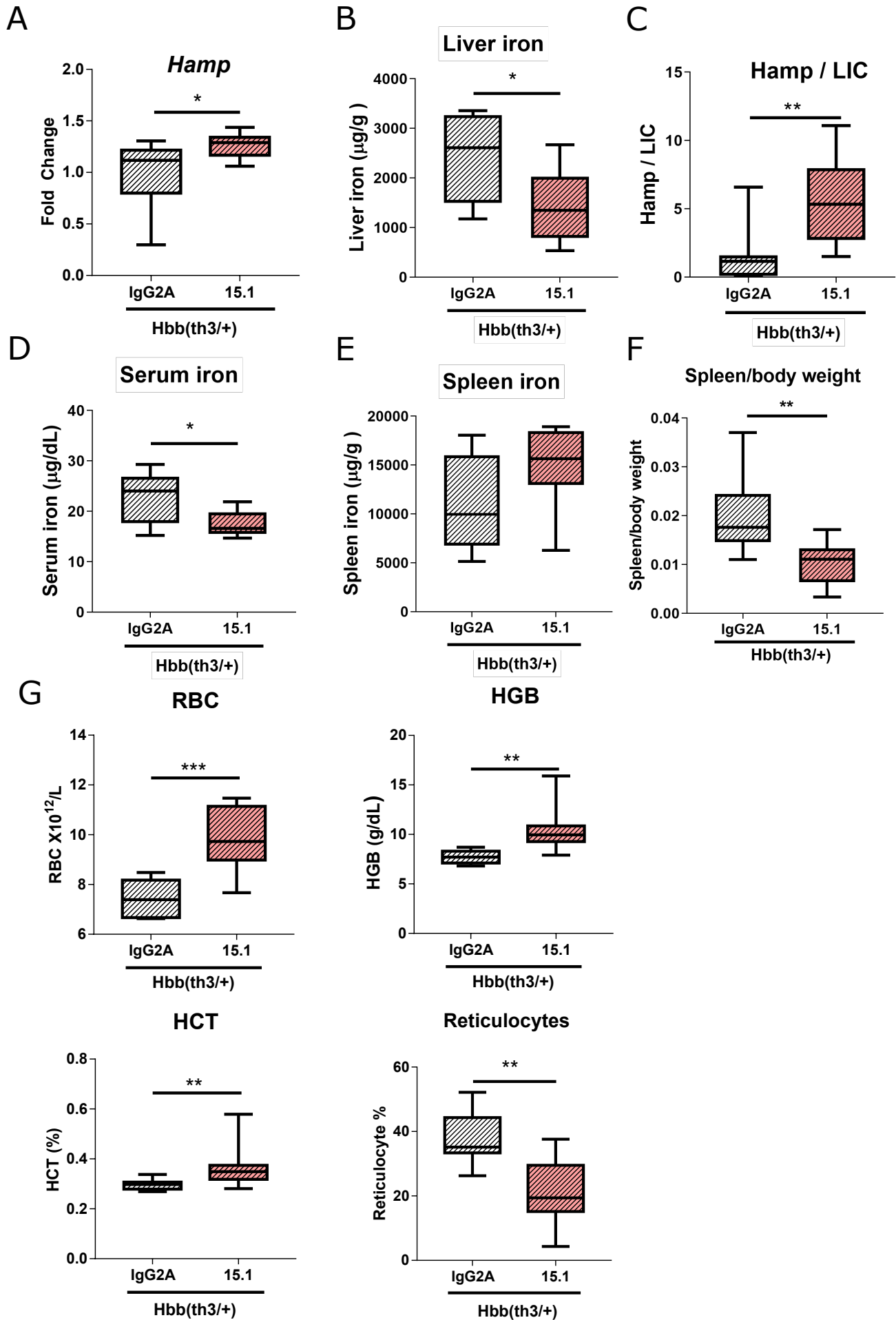


# Figure 6



## **SUPPLEMENTAL INFORMATION FOR**

### **Antibodies against the erythroferrone N-terminal domain prevent hepcidin suppression and ameliorate murine thalassemia**

João Arezes<sup>1\*</sup>, Niall Foy<sup>2\*</sup>, Kirsty McHugh<sup>3</sup>, Doris Quinkert<sup>3</sup>, Susan Benard<sup>4</sup>, Anagha Sawant<sup>5</sup>, Joe N. Frost<sup>1</sup>, Andrew E. Armitage<sup>1</sup>, Sant-Rayn Pasricha<sup>1,6,7</sup>, Pei Jin Lim<sup>1</sup>, May S. Tam<sup>5</sup>, Edward Lavallie<sup>5</sup>, Debra D. Pittman<sup>5</sup>, Orla Cunningham<sup>2</sup>, Matthew Lambert<sup>2</sup>, John E. Murphy<sup>5</sup>, Simon J. Draper<sup>3\*</sup>, Reema Jasuja<sup>5\*</sup> and Hal Drakesmith<sup>1,8\*</sup>

## Supplementary methods

### Antibody discovery: Mouse Hybridoma approach

Ten-to-twelve week old male ERFE KO mice were injected i.p. with 50µg/dose of monoFc-hu on days 0, 14, 28 and 42. Mice were euthanized on day 45 and the spleen harvested for hybridoma production using the ClonaCell-HY Hybridoma kit (StemCell technologies) following the manufacturer's instructions. Briefly, spleen cells were fused with SP2/O myeloma cells for 16-24h. Hybridomas were selected using the HAT (hypoxanthine-aminopterin-thymidine) method, plated and incubated for 13 days. Colonies (1000-2000) were picked into 96-well plates containing 200 µL of ClonaCell-HY Growth Medium E and incubated for 3 days. Supernatants were screened by ELISA in a 96-well plate coated with monoFc-huERFE or control (at 1µg protein/ml in PBS), and colonies with a positive signal for monoFc-huERFE but negative for the control were selected. The six (sister) clones with the highest signal were selected, expanded in DMEM, 10% ultra low IgG FBS, 2mM L-glutamine, 100 U/ml penicillin and 0.1mg/ml streptomycin. Cell culture supernatants were loaded onto Protein G Agarose Pierce columns (2ml per column). IgGs were eluted with 10ml 100mM glycine, pH 2.7; buffered immediately with 350µl 1M Trizma hydrochloride solution pH 9.0 (Sigma) and buffer exchanged into PBS using an Amicon Ultra-15 Ultracel 30K centrifugal filter (Merck). Purified IgGs were sequenced and cloned in to mammalian expression vectors as described previously<sup>26</sup>. Transiently transfected HEK293 cells expressing anti-ERFE were cultured in FreeStyle™ 293 medium or Expi293™ medium (ThermoFisher). These cells were pre-seeded in a wave bioreactor at a cell density of  $1.25 \times 10^6$  cells/ml and transfected with polyethylenimine (Polysciences). The wave bioreactors were incubated at 37 °C with a rocking rate of 20 rpm for 120 h before harvest. The conditioned media was centrifuged using a Sorvall BIOS 16 Bioprocessing Centrifuge (Thermo Fisher Scientific) and filtered with a 0.22 µm filter device prior to purification. The clarified conditioned media was loaded onto a 5 ml MAbSelect SuRe column (GE Life Sciences) equilibrated with PBS, pH 7.2. The column was washed with 10 column volumes of PBS, pH 7.2 before the protein was step eluted using a low pH buffer. The protein was immediately loaded onto a 320 ml Superdex 200 size exclusion column (GE Life Sciences) equilibrated in PBS, pH 7.2. Peak fractions were pooled and filtered through a 0.2µm PES filter. A monoclonal antibody that bound both mouse and human ERFE proteins, and neutralized the ability of both mouse and human ERFE proteins to suppress hepcidin in vitro, was then selected for further use.

### Homogeneous Time Resolved Fluorescence

A competition HTRF assay<sup>29,30</sup> was established in order to assess whether BMPs could compete with neutralising anti-ERFE antibodies for binding to the same/overlapping epitope on recombinant ERFE protein. Anti-ERFE antibody were labelled with europium cryptate using a cryptate labelling kit (CisBio) according to the manufacturer's instructions. The final reaction mix contained 7 nM biotinylated monoFc-human ERFE, 1:1000 dilution of Streptavidin-XL665 (CisBio), 1:300 dilution of the europium cryptate-labeled anti-ERFE antibody, and BMPs or unlabelled anti-ERFE mAb at differing concentrations, in a total reaction volume of 20 µl in 1× assay buffer [50 mM sodium phosphate, pH 7.5, 400 mM potassium fluoride, and 0.1% BSA (w/v)]. Reagents were added sequentially into 384-well low-volume black plates (Nunc). Reactions were allowed to proceed for 3 h at room



temperature, and plates were subsequently read on the EnVision Multilabel Plate Reader (Perkin-Elmer) with excitation at 340 nm and two emission readings at 615 nm (measuring input donor fluorescence from antiERFE antibody-europium cryptate) and 665 nm (measuring output acceptor fluorescence from Streptavidin-XL665). All readings were expressed as the percentage of change in fluorescence, % $\Delta F$ , where: % $\Delta F = [(F665 \text{ Sample}/F615 \text{ Sample}) - (F665 \text{ Control}/F615 \text{ Control})] / (F665 \text{ Control}/F615 \text{ Control}) \times 100$ . Data plotted as “% Control” representing the background fluorescence energy transfer in wells containing 1:1000 of each labelled antibody, in assay buffer, alone.

## **ELISA**

Maxisorp plates (Nunc) were coated with 1  $\mu\text{g/ml}$  of the indicated antigens in PBS overnight at 4 °C. Wells were washed three times with 300  $\mu\text{l}$  of PBS containing 0.05% (v/v) Tween-20, and blocked in 200  $\mu\text{l}$  of blocking buffer (PBS/3% (w/v) milk with 1% BSA (w/v)) for 1 h. Plates were washed three times with 300  $\mu\text{l}$  of PBS containing 0.05% (v/v) Tween-20. Relevant test antibodies were serially diluted in blocking solution in a separate plate and added to the ERFE-coated plates and incubated, rocking for one hour at RT. Plates were washed as previously and peroxidase conjugated goat anti-mouse Fc secondary antibody was added to each well at a 1:2000 dilution in blocking buffer. Plates were incubated with rocking at RT for one hour prior to a final washing step. The reaction was developed by addition of 75  $\mu\text{l}$  per well of UltraTMB (Pierce) and stopped by addition of an equal volume of 0.18 M phosphoric acid. The plates were read in an Envision Multiplate reader at 450nm. Data was plotted using Prism 5 software (Graphpad). Serum hepcidin was quantified by competitive ELISA using the Hepcidin-Murine Compete Kit (Intrinsic Lifesciences) according to the manufacturer’s protocol.

## **RNA isolation, cDNA synthesis and qRT-PCR**

Liver (preserved in RNA later prior to lysis using a TissueRuptor(Qiagen) or cells were lysed and RNA was isolated using the RNeasy Plus kit (Qiagen), followed by RNA quantification and quality assessment using Nanodrop (Thermo Fisher). cDNA was synthesized using the High Capacity RNA-to-cDNA kit (Applied Biosystems). Gene expression was assessed using quantitative real-time PCR with Taqman Gene Expression Master Mix and inventoried Taqman Gene expression assays (Applied Biosystems) specific for the genes of interest (supplementary table 1). *GAPDH* or *Hprt1* were used as endogenous control genes for human cells and mouse tissues respectively, and qPCR was performed using the QuantStudio 7 Flex Real-Time PCR system.

## **Tissue non-heme iron measurement**

Liver and spleen tissues were dried for 4 hours at 100 °C, weighed and digested in 10% trichloroacetic acid (Sigma)/ 30% hydrochloric acid (Sigma) for 20 hours at 65 °C. A standard curve was generated using a dilution series of ferric ammonium citrate (Sigma) in the 10% (w/v) trichloroacetic acid/ 30% hydrochloric acid mixture. Non-heme iron content was determined colorimetrically by measuring absorbance at 535nm following reaction with chromogen reagent containing 0.1% (w/v) bathophenoldisulphonic acid (Sigma) / 0.8% thioglycolic acid (Sigma).

**Blood parameters, serum iron and serum transferrin analysis**

Blood was taken by cardiac puncture immediately after euthanising mice and collected in BD EDTA or SST (serum) Microtainer tubes. Whole EDTA-blood was immediately used for quantification of blood parameters using a hematology analyser (Sysmex KX-21-N or IDEXX Procyte Dx). Serum was prepared by centrifugation of clotted blood at 8000 x g for 3 minutes in BD Microtainer SST tubes (Beckton Dickinson) and used for serum iron and serum transferrin quantification using a Abbott Architect c16000 automated analyzer (Abbott Laboratories)

Protein	Species	Gene	Assay code
Glyceraldehyde 3-phosphate dehydrogenase	Human	<i>GAPDH</i>	Hs99999905_m1
Hepcidin	Human	<i>HAMP</i>	Hs00221783_m1
Inhibitor of DNA-binding protein 1	Mouse	<i>Id1</i>	Hs03676575_s1
Inhibitor of DNA-binding protein 2	Mouse	<i>Id2</i>	Hs00171409_m1
Atonal BHLH Transcription Factor 8	Mouse	<i>Atoh8</i>	Mm00464055_m1
Sons of mothers against decapentaplegic 7	Mouse	<i>Smad7</i>	Mm00484742_m1
Bone morphogenetic protein 2	Mouse	<i>Bmp2</i>	Mm01340178_m1
Bone morphogenetic protein 6	Mouse	<i>Bmp6</i>	Mm01332882_m1
Hepcidin	Mouse	<i>Hamp1</i>	Mm04231240_s1
Hypoxanthine-guanine phosphoribosyltransferase	Mouse	<i>Hprt1</i>	Mm01545399_m1

### Supplementary Table 1

Assay codes for Taqman Gene expression assays specific for the genes of interest

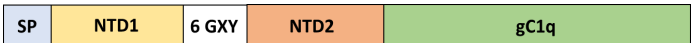
**Figure S1: The globular C1q domain of ERFE is not sufficient to suppress hepcidin. (A)** structure of full length ERFE and globular C1q domain **(B)** Huh7 cells were treated for 24h with 1µg/ml of full length ERFE or the globular C1q domain of ERFE, and analysed for *HAMP* gene expression. Columns represent mean + standard deviation. n=3 replicates per group \*\*\*\*P<0.001 using Student t test.

**Figure S2:** Eight-weeks old male C57BL/6 mice were treated intraperitoneally with 200 units of erythropoietin (EPO) once per day for three consecutive days, in combination with intravenous injections of 400 µg of an IgG antibody control, anti-ERFE 15.1 or anti ERFE 20.1 on day 1 and day 3 (or vehicle alone instead of EPO for analysis of baseline values). Anti-ERFE 15.1 and 20.1 were tested in independent experiments. Mice were euthanized and analysed 24h after the last treatment for analysis of liver *Hamp* expression **(A)**, serum and liver iron **(B)**, and blood parameters **(C)**. n= 3 (vehicle), 5 (EPO + IgG) or 6 (EPO + anti-ERFE). \*P<0.05; \*\*P <0.01; \*\*\*P<0.001; \*\*\*\*P<0.0001 one-way ANOVA followed by Tukey's test.

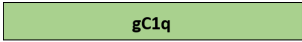
# Figure S1

A

Full length ERFE



C1q ERFE



B

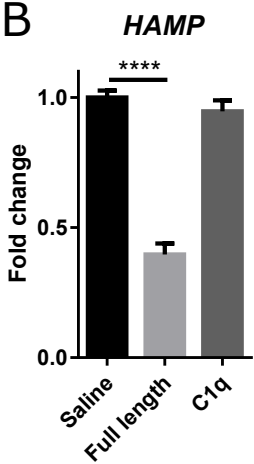


# Figure S2

